Design and Analysis of a Flat Plate Solar Powered Ejector Refrigeration System

Hani Sait[1,*], Badr Habeebullah[2], Nadim Turkman[2], Yasin Al Khatib[2] and Ahmad Hussain[2]

[1]King Abdulaziz University, Rabigh, Saudi Arabia and [2]King Abdulaziz University, Jeddah, Saudi Arabia

Abstract: The Ejector refrigeration system can operate using renewable energy such as solar or wasted heat. A mathematical model for an ejector refrigeration system powered by solar energy was developed. The Ejector refrigeration system depends on many factors, such as ejector geometry, NXP, and operating conditions. A flat plate solar collector is designed to predict the heat transfer performance for the whole system, and the primary factors affecting the heat transfer performance. Outlet temperature of 134.95 °C was achieved from the setup of five solar collectors (two square meters each) when the solar irradiance was 985.69 W/m^2. The water needs total power of 5016 W to reach this temperature.

Key Words: Ejector, Solar, Flat plate, Evacuated tube.

1. INTRODUCTION

The ejector refrigeration system was first invented in 1939, [1] and improved between 1942 to 1950 when the mixing concept at constant pressure was introduced, [2]. Ejector Refrigeration System (ERS) has the advantage that it can be powered by low-grade energy, renewable or waste heat that can be supplied at a low cost. Also, ERS is reliable because it does not require a motor and has no exhaust to the environment [2-8].

Several issues were raised for ERS, such as the primary nozzle and ejector geometry, type of the working fluid, temperatures of the boiler, and the evaporator. The behavior of the fluid as it passes through the nozzle is also another issue [9-23].

The Ejector Refrigeration Cycle is similar to the conventional vapor compressor cycle, except the compressor is replaced by a boiler and ejector. The ERC is shown in Figure **1** consists of a boiler, an evaporator, a primary ejector or nozzle, a convergent-divergent nozzle, a condenser, and a feeding pump. The low pressure is created by the high-speed exit from the primary ejector causing the secondary flow to occur and suck the vapor from the evaporator. The pressure of the combined flow in the boiler and the evaporator will increase, causing a heat release in the condenser. The condensed liquid is pumped back to the boiler, the evaporator, and the cycle is repeated. The ejector refrigeration cycle attracts attention because of its simplicity and ability to utilize waste heat, which is available in most factories and vehicles [24-33].

Figure **2** shows the ejector cross-section and pressure and velocity profiles through it. The primary fluid accelerates through the primary nozzle to exit as supersonic flow when entering the convergent-divergent nozzle. Low pressure is then created at the nozzle exit, which sucks the vapor. The evaporator pressure falls, letting the boiling occurs at low temperature. Both flows are mixed in the convergent-divergent nozzle. The shock wave occurs at the diffuser's entrance, causing a sudden rise in the pressure, which allows the flow to continue flowing to the condenser.

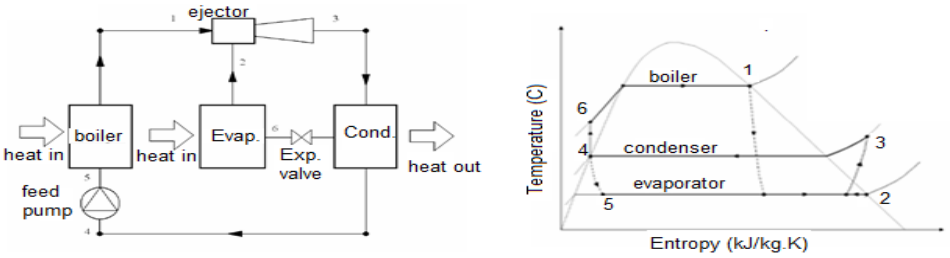

Figure 1: Steam ejector cycle and the corresponding T-s diagram.

*Address correspondence to this author at the King Abdulaziz University, Rabigh, Saudi Arabia; Email: hhsait@kau.edu.sa

 © 2020 Avanti Publishers

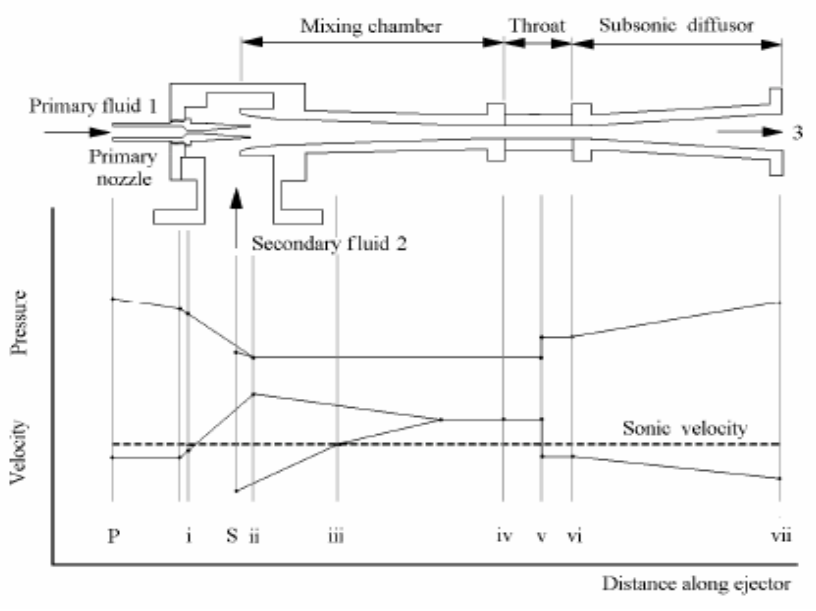

Figure 2: Ejector cross-section and pressure and velocity profiles through it.

2. UTILIZING SOLAR ENERGY FOR EJECTOR REFRIGERATION SYSTEM

Saudi Arabia is one of the richest countries with solar energy. The rate of the irradiation can reach up to 2500 kWh/m2/y, as shown in Figure **3** [34].

The temperature variations in Jeddah through the year is shown in Figure **4**. The maximum temperature appears to be in July at 39.4°C, where the minimum temperature appears in January at 20°C. The daily range is about 10°C in winter and 13°C in summer.

The relative humidity affects the heat flux from the sun. Humidity usually reduces the solar intensity which makes it an unwanted factor for utilizing the sun. Figure **5** shows the relative humidity for Jeddah throughout the year.

In an ejector type refrigeration system assisted by solar energy, the changes in solar radiation energy make it challenging to sustain a constant temperature in the generator. Ejector with a more massive solar collector and throat area enables a more extensive working scale of generator temperatures but may be oversized and costly. The basic types of thermal solar collectors can be either flat plate or evacuated tube as shown in Figure **6**.

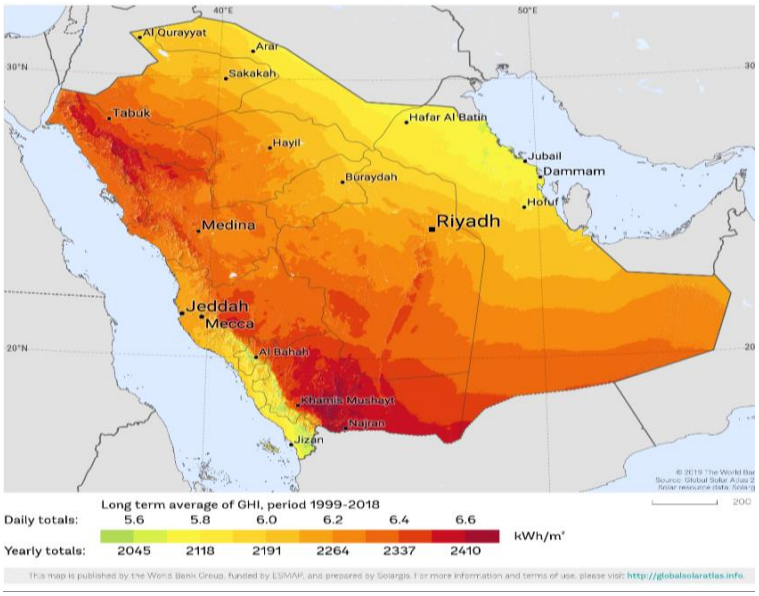

Figure 3: Thermal map of solar distribution in Saudi Arabia.

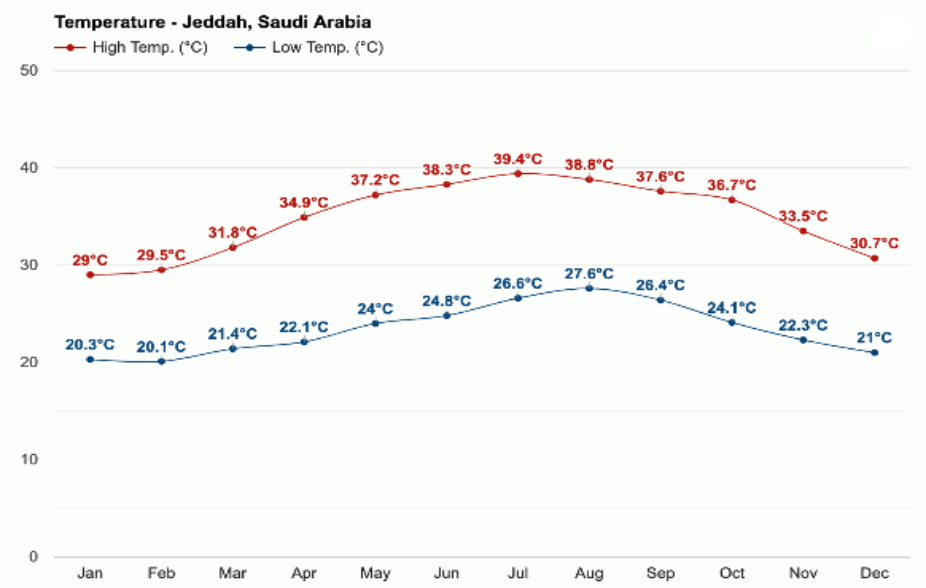

Figure 4: Temperature variation during throughout the year in Jeddah,Saudi Arabia "Weather atlas.com".

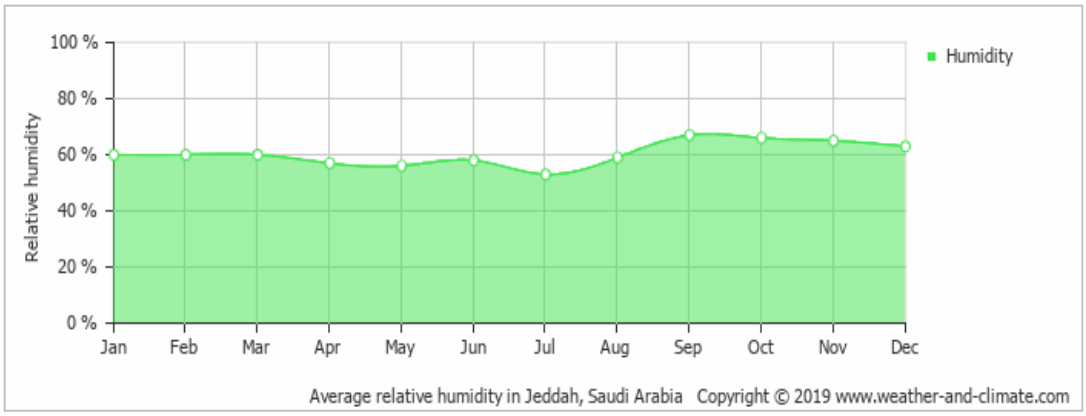

Figure 5: Relative humidity variation throughout the year, "weather-and-climate.com".

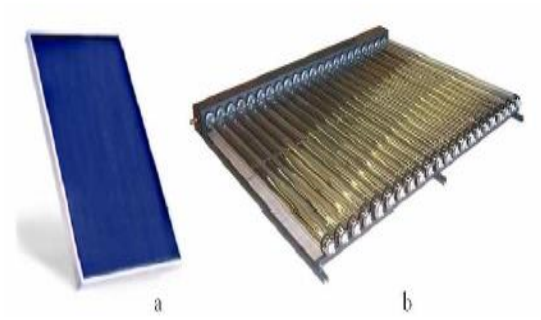

Figure 6: Solar thermal collector types, (a) Flat plate solar collector, (b) Evacuated tube, solar collector.

On the other hand, reducing the throat area narrows the working scale of generator temperatures. Hence the ejector with a rigid throat area may be inappropriate to utilize heat from solar energy [8] when the generator temperature in ERS ranges between 120-140 °C. The efficiency of these systems decreases when used with solar to generate refrigerant vapor due to the reduction of solar collector's efficiency at elevated temperatures. Therefore, the ERS system utilizing solar energy as a heat input requires relatively low generator temperatures and, at the same time, should use environmentally friendly refrigerants [35].

The Solar-driven Ejector Refrigeration system (SER) was investigated widely by many authors [8, 19, 35-38] [3-10]. The optimization of the performance of an adjustable throat ejector in a solar refrigeration system was done by Yen, R.H. *et al*. [8]. A curve-fitting correlation relates to the optimum ratio of the throat area with the working temperatures was derived. Using this relation to set the throat area ratio, the ejector can consistently reach stable and optimal performances under a changing solar heat supply. They concluded that if any of the condenser, evaporator, or generator temperature is known, the ejector could be set to the equivalent optimal ratio of throat area using the correlation equation [8].

The use of both solar energies as low-grade heat and eco refrigerants is also a primary concern. The matter will be more challenging when trying to utilize a low-temperature heat source in the range of 80 °C or lower.

The SER system assisted by the low-temperature heat source was studied by Dong, J *et al*. [19]. Several parameters' effects on the performance of the ejector, including the operating temperature, the nozzle exit position (NXP), and the constant area section's diameter, were studied at an additional low-temperature heat source. They found that the steam ejector can function for a selected size configuration of the steam ejector with a generator temperature varying between 40°C up to 70°C and an evaporator temperature of 10°C.

Ma X. *et al*. [35] studied the steam ejector refrigerator with a cooling capacity of 5 kW fit for solar energy utilization. A spindle was used to control the ejector's primary flow to provide fine-tuning for ejector operation and best COP. They got a COP of 0.32 for the ejector cooling system during the test at a boiler temperature around 90 °C. A COP up to 0.16 was predicted for the combined system in operation.

The SER system under various working situations was investigated by Evangelos Bellos and Christos Tzivanidis [39]. Various evaporator temperatures from -10°C to 10°C and various heat rejection temperatures from 30°C to 50°C were investigated. They found that R141b is the best selection in all operating situations. The maximum COP was found to be 0.234 when the evaporator temperature at 10°C and heat is rejected to the environment at 30°C. The refrigeration production ranged from 1.85 kW to 23.39kW, while the optimum generator temperatures were found to be from 114°C to 157°C.

Allouche, Y *et al*. [36] studied a Solar-Assisted ERS for Mediterranean Climate. They observed that the system needs to have a deep vacuum to make the system perform as predicted by the theoretical studies. They had an ejector working continuously at a real scale under real operational conditions.

The performance of an Ejector Air-conditioning Cycle with Solar energy using heavy hydrocarbons as refrigerants was investigated by Gil, B. and J. Kasperski [38]. Pentane (R601) and Hexane (R602) were selected as working fluids. The COP, obtained for refrigerants R601 and R602, were 0.1 and 0.5, respectively, at operation conditions of Te=12°C, Tc=30°C, and solar intensity of 800 W/m^2. The selected range for the generator temperature was 100–190°C for Pentane (R601) and 100–200°C for Hexane (R602).

Diaconu, B.M [40] conducted an energy analysis of a solar-powered ejector air conditioning system that stores cold water in thermal energy storage connected to the evaporator to ensure consistent operating conditions ejector cycle. He achieved a COP of 0.45 for a cold thermal storage capacity of 5 kW.

Experimental investigations of a solar-driven ejector A/C system with isobutane as a refrigerant under motive vapor temperature below 75◦C was tested by Śmierciew, K *et al*. [41]. They found that the investigated setup's loss coefficient was over 0.75 with motive heat-source below 80◦C.

The solar driven ejector refrigeration system can be utilized widely in a country rich with solar irradiation such as Saudi Arabia. There are still many issues that need to be resolved such as the minimum working temperature of the boiler, refrigerant types and enhancing the COP. In this project, an analytical approach was conducted to design the solar collector, driving the ejector refrigeration system. An experimental attempt to use a vacuum tube solar water heater to generate steam for the ejector boiler was tried.

3. MATHEMATICAL MODEL FOR SOLAR DRIVEN REFRIGERATION SYSTEM

The basic ejector refrigeration system, shown in Figure **1**, consists of a generator (high-temperature evaporator—sometimes called a boiler), a low-temperature evaporator, a primary nozzle, a convergent-divergent ejector, a condenser, and a pump. The generator forms high-pressure steam, which is delivered to the primary nozzle. The primary steam exits from the primary nozzle, as shown in Figure **1** at high speed, and forms a vacuum area that allows suction of the secondary steam from the evaporator, creating low pressure and low-temperature area, the two fluids mixed in the mixing zone in the convergent part of the ejector. The mixed fluid continues its way towards the condenser passing by the constant area and the divergent section of the ejector. The liquid then releases heat to the condenser and is split into two portions. The primary fluid is pumped into the generator, while the secondary fluid is suctioned up by the low-pressure evaporator.

The coefficient of performance (COP) of the ERS is given by:

$$\boldsymbol{COP} = \frac{\text{useful refrigeration}}{\text{heat input to HTE + power consumed by pump}} \quad (1)$$

The pump's required power can be ignored since it is much smaller than the heat input to the boiler and then Eq. (1) can be rewritten as:

$$\boldsymbol{COP} = \frac{\dot{m}_{sf} h_{fg,sf}}{\dot{m}_{pf} h_{fg,pf}} \quad (2)$$

where h_{fg} is the latent heat of vaporization and $\dot{m}$ is the mass flow rate at the individual evaporators. If the secondary liquid is the same as the primary liquid, Eq. (2) would almost decrease to being proportionate to the entrainment proportion, i.e.,

$$\boldsymbol{COP} = \frac{\dot{m}_{sf}}{\dot{m}_{pf}} \quad (3)$$

4. THE SOLAR COLLECTORS: MODELING AND DESIGNING

Solar-powered ejector types can be one of the following direct heating, closed-loop, or open loop as shown in Figure **7**.

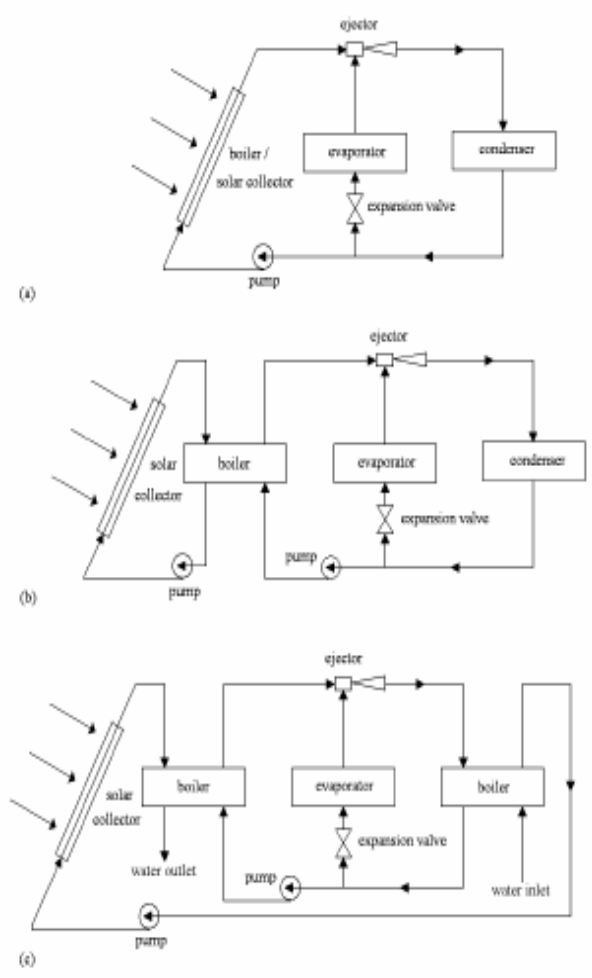

Figure 7: Solar-powered ejector types: (a) direct heating, (b) closed-loop, (c) open loop.

4.1. Solar and Collector Geometrical Parameters

Flat plate solar collectors will be modeled using the methodology given by Rabl [11].

Solar and collector geometrical parameters are as follows:

a) I_o: Solar constant:

$$I_o = 1372.7\ W/m^2 \quad (4)$$

b) $I_{o,e}$: Effective solar constant: With the day of the year, n, it is given as:

$$I_{o,e} = \left[1 + 0.033\, cos\left(\frac{360\, n}{365.25}\right)\right] I_o \quad (5)$$

c) δ: Declination angle:

$$sin\ \delta = -sin\ 23.45\ cos\left[\frac{360(n+10}{365.25}\right] \quad (6)$$

ω: Hour angle: With the solar time of the day, $t_d(h)$, it is given as:

$$\omega = 180(12 - t_d)/12 \quad (7)$$

d) ω_s: Sunset hour:

$$cos\ \omega_s = -\,tan\,\lambda\, tan\,\delta \quad (8)$$

θ: Collector incidence angle: With the collector tilt angle, and β the latitude angle

$$cos\,\theta = cos(\beta - \lambda)\, cos\,\delta\, cos\,\omega - sin(\beta - \lambda)\, sin\,\delta \quad (9)$$

$I_{o,h}$: The the extraterrestrial solar irradiance on a horizontal surface, $I_{o,h}$, is given as:

$$I_{o,h} = I_{o,e}\, cos\,\lambda\, cos\,\delta\ (cos\,\omega - cos\,\omega_s) \quad (10)$$

H_o: The daily extraterrestrial solar irradiance on a horizontal surface, $\mathrm{H_o}$, is given as:

$$H_o = \frac{24}{\pi} I_{o,e}\, cos\,\lambda\, cos\,\delta \left(sin\,\omega_s - \frac{\pi}{180}\omega_s cos\omega_s\right) \quad (11)$$

I: The global solar irradiance on a tilted surface is given as [1]:

$$I = I_b cos\,\theta + I_d \frac{(1+cos\,\beta)}{2} + I_h \rho_g \frac{(1-cos\,\beta)}{2} \quad (12)$$

Where I_b, I_d, and I_h are beam irradiance, diffuse irradiance, and hemispherical irradiance respectively, while ρ_g is ground reflectivity assumed as 0.2.

4.2. Solar Radiation Calculation Using Clear Sky Model

a) I_b: Beam irradiance is given with zenith angle,θ_z, as [15]:

$$I_b = I_{o,e}\left[a_o + a_1 exp\left(-\frac{k}{cos\,\theta_z}\right)\right] \quad (13)$$

$$a_o = r_o[0.4237 - 0.00821(6 - H)^2] \quad (14)$$

$$a_1 = r_1[0.5055 + 0.00595(6.5 - H)^2] \quad (15)$$

$$k = r_k[0.2711 + 0.01858(2.5 - H)^2] \quad (16)$$

$$cos\ \theta_z = cos(\lambda)\ cos\ \delta(cos\ \omega - cos\ \omega_s) \quad (17)$$

H is the elevation above the sea (km) and correction factors $r_o = 0.97$, $r_1 = 0.96$ and $r_k = 1.02$ for midlatitude summer climate conditions.

I_d: The diffuse irradiance is given as [16]:

$$I_d = \left(0.271I_{o,e} - 0.2939I_b\right) cos\ \theta_z \quad (18)$$

I_h: The hemispherical irradiance is given as :

$$I_h = I_b\ cos\ \theta_z + I_d \quad (19)$$

4.3. Solar Radiation Calculation Using Given Daily Hemispherical Irradiance

b) K_T: The average clearness index for the month: With a given the monthly average of daily hemispherical irradiance,H_h, it can be found as:

$$K_T = \frac{H_h}{H_{o,e}} \quad (20)$$

H_d: The monthly average of daily diffuse irradiance: it can be found as [17]:

$$\frac{H_d}{H_h} = 0.775 + \frac{0.347(\omega_s - 90)\pi}{180} - \left[0.505 + \frac{0.261(\omega_s - 90)\pi}{180}\right] \cos[360\,\frac{K_T - 0.9}{\pi}] \quad (21)$$

I_d: The diffuse irradiance: It is given as:

$$r_d = \frac{\pi}{24}\frac{cos\ \omega - cos\ \omega_s}{sin\ \omega_s - \left(\frac{\pi\omega_s}{180}\right) cos\ \omega_s} \quad (22)$$

$$I_d = r_d H_d \quad (23)$$

I_h: Hemispherical irradiance: it is given as:

$$a = 0.4090 + 0.5016\ sin(\omega_s - 60^o) \quad (24)$$

$$b = 0.6609 - 0.4767\ sin(\omega_s - 60^o) \quad (25)$$

$$I_h = (a + b\ cos\ \omega) r_d H_h \quad (26)$$

I_b: Beam irradiance: It is given as:

$$I_b = \frac{I_h - I_d}{cos\ \theta_z} \quad (27)$$

4.4. The Optical Efficiency of the Solar Collector

c) τ: Average transmittance of the double (*N=2*) glazing is obtained from Fresnel equations [12].

$$\theta_c = asin\ (\frac{1}{n} sin\ \theta) \quad (28)$$

$$r_{\parallel} = \frac{tan^2(\theta - \theta_c)}{tan^2(\theta + \theta_c)}, \quad r_{\perp} = \frac{sin^2(\theta - \theta_c)}{sin^2(\theta + \theta_c)} \quad (29)$$

$$\tau = \frac{1}{2}\left[\frac{1 - r_{\perp}}{1 + (2N - 1)r_{\perp}} + \frac{1 - r_{\parallel}}{1 + (2N - 1)r_{\parallel}}\right] \quad (30)$$

Where n is the relative refraction index of glass and air, which is assumed as 1.5.

The optical efficiency of the double (*N=2*) glazing is given as:

$$\eta_o = \frac{\tau\alpha}{1 - (1 - \alpha)\rho_d} \quad (31)$$

Where α is absorber plate absorptance and ρ_d is diffuse reflectance, both are assumed constant values of 0.9 and 0.2.

4.5. The Heat Transmission in the Solar Collector

Heat losses from the collector, Q_l, is defined as:

$$Q_{sc,l} = U_{sc,l} A_p (T_p - T_a) \quad (32)$$

U_{sc} is the overall heat loss coefficient, A_p is the absorber plate area, T_p is the average temperature of the absorber plate, and T_a is the ambient temperature.

The overall heat loss coefficient, $U_{sc,l}$, is defined as:

$$U_{sc,l} = U_{sc,f} + U_{sc,b} + U_{sc,s} \quad (33)$$

Where $U_{sc,f}$ is the coefficient of heat loss from the absorber plate to the outside air via the glass covers, $U_{sc,b}$ is the heat loss coefficient from the plate of the absorber to the ambient air through the insulation and $U_{sc,s}$ is the amount of heat loss coefficient between the absorber plate and the outside air via the side insulation.

$U_{sc,b}$ is defined as:

$$U_{sc,b} = \frac{k_{sc,i}}{t_{sc,i}} \quad (34)$$

Where $k_{sc,i}$ is the thermal conductivity of the insulation material, which is selected as 0.038 (glass wool) [13], while $t_{sc,i}$ is the thickness of the insulation selected 0.05 m.

$U_{sc,s}$ is defined as:

$$U_{sc,s} = \frac{k_{sc,i}}{t_{sc,i}}\frac{A_{sc,s}}{A_{sc,p}} \quad (35)$$

Where, $A_{sc,s}$ is the total side area of the collector.

$U_{sc,f}$ is obtained as a result of curve fitting as [4] for $\beta \leq 70^o$:

$$f = (1 + 0.089h_{sc,a} - 0.1166h_{sc,a}\varepsilon_p)(1 + 0.07866N) \quad (36)$$

$$A = \frac{520(1 - 0.000051\ \beta^2}{T_p}\left[\frac{T_p - T_a}{N + f}\right]^{0.43(1 - \frac{100}{T_p})} \quad (37)$$

$$B = \frac{1}{\epsilon_p + 0.00591Nh_{sc,a}} + \frac{2N + f - 1 + 0.133\ \epsilon_p}{\epsilon_c} \quad (38)$$

$$U_{sc,f} = \left[\frac{N}{A} + \frac{1}{h_{sc,a}}\right]^{-1} + \frac{\sigma(T_p+T_a)(T_p{}^2+T_a{}^2)}{B-N} \quad (39)$$

where ϵ_c and ϵ_p are the glazing cover emissivity, which is assumed 0.88 for both covers and emissivity of the absorber plate considered as 0.1. Stefan–Boltzmann constant σ is 5.67E−8 W/ m^2 K^{4}and h_a is the coefficient of heat transfer from the surface of the collector to the ambient which can be found from Nusselt Numbers as:

$$Re = \frac{V_a l_e}{\upsilon} \quad where \;\; l_e = \frac{4WL}{2(W+L)} \quad (40)$$

$$Nu = 0.86Re^{1/2}Pr^{1/3}, \;\; 20{,}000 \leq Re \leq 100{,}000 \quad (41)$$

$$Nu = 0.036(Re^{0.8} - 23{,}200)Pr^{1/3}, \;\; 500{,}000 \leq Re \quad (42)$$

$$h_{sc,a} = \frac{Nuk_a}{l_e} \quad (43)$$

Where *W* and *L* are the collector's width and length, V_a is the air velocity over the collector, υ is the kinematic viscosity at film temperature, and l_e is the equivalent length.

Fin efficiency of the collector, *F*, is defined as:

$$m = \sqrt{\frac{U}{k_p t_p}} \quad (44)$$

$$F = \frac{tanh\, mw}{mw} \quad (45)$$

Where k_p and t_p are the absorber plate thermal conductivity and thickness, respectively, which selected as 401 W/mK (copper), 0.001 m, while *w*=0.05 m is the length of the fin for each pipe.

The solar collector parameter, F_m, is defined as [14]:

$$F_m = \frac{1}{\frac{d+2w}{d+2Fw} + \frac{(d+2w)U}{\pi d_i h_i}} \quad (46)$$

Where d the outer diameter of the collector pipe, d_i is the inner diameter of the collector pipe and h_i is the coefficient heat transfer from the pipe's inner surface to the water, calculated using:

$$Re = \frac{V_w d_i}{\upsilon} \quad (47)$$

$$Nu = 3.66 \; for \; Re \leq 2300 \quad (48)$$

$$Nu = \frac{\left(\frac{f}{8}\right)(Re-1000)Pr}{1+12.7\left(\frac{f}{8}\right)^{\frac{1}{2}}\left(Pr^{\frac{2}{3}}-1\right)} \; for \; Re \geq 2300 \quad (49)$$

$$h_{sc,i} = \frac{Nu\, k}{d_i} \quad (59)$$

Where V_w is the water velocity inside the tube, $\upsilon \; and \; k$ are the kinematic viscosity and the thermal conductivity at film temperature, and *f* is the friction coefficient and is calculated as:

$$f = \frac{64}{Re} \; Re \leq 2300 \quad (51)$$

$$\frac{1}{\sqrt{f}} = -2.0log\left[\frac{e/D}{3.7} + \frac{2{,}51}{Re\sqrt{f}}\right] \quad (52)$$

Heat transfer factor of the collector, F_{in}, is defined as [14]:

$$F_{in} = \frac{\dot{m}_{sc}c_{sc}(T_{out}-T_{in})}{A_p(\eta_o I - U(T_{in}-T_a))} \quad (53)$$

and is found as:

$$F_{in} = \frac{\dot{m}_{sc}c_{sc}}{U_{sc,l}A_p}\left[1 - exp\left(-\frac{F_m U_{sc,l}A_p}{\dot{m}_{sc}c_{sc}}\right)\right] \quad (54)$$

Where $\dot{m}_{sc}c_{sc}$is the heat capacity of the water, T_{in} is the temperature of the inlet water, and T_{out} is the outlet water temperature.

The collector outlet temperature of the water, T_{out}, is found as:

$$T_{out} = T_{in} + \frac{F_{in}A_p(\eta_o I - U_{sc,l}(T_{in}-T_a)}{\dot{m}_{sc}c_{sc}} \quad (55)$$

Energy gain, q is found as:

$$Q_{sc} = A_p\left[\eta_o I - U_{sc,l}\left(T_p - T_a\right)\right] = \dot{m}_{sc}c_{sc}(T_{out} - T_{in}) \quad (56)$$

Absorber plate temperature, T_p, will be iteratively calculated as:

$$T_p = T_a + \frac{A_p\eta_o I - \dot{m}_{sc}c_{sc}(T_{out}-T_{in})}{U_{sc,l}A_p} \quad (57)$$

Then, the efficiency of the collector, η, will be as:

$$\eta = F_{in}\left[\eta_o - U_{sc,l}(T_{in} - T_a)/I\right] \quad (58)$$

5. RESULTS AND DESIGN PARAMETERS

Five flat-plate solar collectors were connected in serial as a source of heat to the system. Water enters each collector at a fixed flow rate and was divided into nine copper tubes in each collector. The constant geometrical parameters of the solar collector are shown in Table **1**, while the operational conditions are illustrated in Table **2** as the fixed design parameters. In Table **3**, other design parameters that were calculated iteratively are given.

It has been shown that an outlet temperature of 134.95 °C can be achieved from the setup of five solar collectors when the solar irradiance is 985.69 W/m^2. The water needs total power of 5016 W to reach this temperature. It is expected that these results will vary in the summertime when the irradiation will be much higher.

The thermal energy from the temperature difference between the evaporator and condenser is the driving force for the solar collector. The average velocity of fluid motion occurring in the system can be calculated for a given temperature difference between the evaporator and condenser.

The Ejector refrigeration system of low generating temperature can be run using solar power. The solar heat supply may vary due to variations in solar radiation intensity, making it challenging to maintain a uniform temperature in the generator. An ejector with a larger throat area and a more massive solar collector allows a more extensive operating range of generator temperatures but may be overdesigned and expensive. An OHP can enhance the solar power of the collector. Nano-fluids can be used to increase the efficiency of the solar collector as well.

Table 1: Parameters of the Solar Collector

Code	Name	Value	Unit	Comments
L	Length of the collector	2.07	m	Selected.
W	Width of the collector	1.04	m	Calculated from other fixed parameters.
H	The thickness of the collector	0.10	m	Selected.
d	Collector tube outside diameter	0.0159	m	1/2", Copper tube, ASTM B88
d_i	Collector tube inside diameter	0.0145	m	1/2", Copper tube, ASTM B88
e	Roughness of tube	1.5E-6	m	Copper tube [19]
w	Half distance between tubes	0.05	m	Selected.
N_t	Number of the tubes	9	-	Selected.
l_i	Insulation thickness	0.1	cm	Glass wool
k_i	Insulation thermal conductivity	0.038	W/m^{2}K	[19]
N_c	Number of the glass covers	2	-	Selected.

Table 2: Design Parameters of the Solar Collector

Code	Name	Value	Unit	Comments
n	Day of the year	80	°C	Selected. (20/03/2020)
t	Time of the day	12:00	noon	Selected. (Solar time)
T_a	Ambient temperature	30	°C	Jeddah solar data
β	The tilt angle of the collector	21.54	degree	Selected. (Latitude of Jeddah)

Table 3: Calculated Design Parameters of the Solar Collector

Code	Name	Value	Unit	Comments
I	Solar irradiance	985.69	W/m^2	On the collector surface
q	Heat transfer to the water	1034	W	
η	Efficiency	0.486		
T_{in}	Inlet water temperature	125.00	°C	In the first collector
T_{out}	Outlet water temperature	127.05	°C	
q	Heat transfer to the water	1019	W	
η	Efficiency	0.478		
T_{in}	Inlet water temperature	127.05	°C	In the second collector
T_{out}	Outlet water temperature	129.08	°C	
q	Heat transfer to the water	1003	W	
η	Efficiency	0.471		
T_{in}	Inlet water temperature	127.08	°C	In the third collector
T_{out}	Outlet water temperature	131.06	°C	
q	Heat transfer to the water	988	W	
η	Efficiency	0.464		
T_{in}	Inlet water temperature	131.06	°C	In the fourth collector
T_{out}	Outlet water temperature	133.02	°C	
q	Heat transfer to the water	972	W	
η	Efficiency	0.457		
T_{in}	Inlet water temperature	133.02	°C	In the fifth collector
T_{out}	Outlet water temperature	134.95	°C	

6. CONCLUSIONS

The Ejector refrigeration system of low generating temperature can be run using solar energy. The solar heat supply may vary because of variations in solar irradiation intensity, making it challenging to maintain a steady generator temperature. It has been shown that an outlet temperature of 134.95 °C can be achieved from the setup of five solar collectors when the solar irradiance is 985.69 W/m^2. The water needs total power of 5016 W to reach this temperature. It is expected that these results will vary in the summertime where the irradiation will be much higher.

An ejector with a greater throat area and larger solar collector allows a wider operating range of generator temperatures but may be overdesigned and expensive. An OHP can enhance the solar power of the collector. Nanotechnology can be used to increase the efficiency of the solar collector as well.

ACKNOWLEDGMENTS

This project was funded by the National Plan for Science, Technology, and Innovation (MAARIFAH)–King Abdulaziz City for Science and Technology—the Kingdom of Saudi Arabia – Award No. 12-ENE3061-03. The authors also acknowledge with thanks the staff at the Science and Technology Unit of King Abdulaziz University in Jeddah for their technical support.

REFERENCES

[1] Sun, D.-W., Comparative study of the performance of an ejector refrigeration cycle operating with various refrigerants. Energy Conversion and Management, 1999. 40(8): p. 873-884.

[2] Varga, S., A.C. Oliveira, and B. Diaconu, Influence of geometrical factors on steam ejector performance – A numerical assessment. International Journal of Refrigeration, 2009. 32(7): p. 1694-1701. http://doi.org/10.1016/j.ijrefrig.2009.05.009

[3] Wang, L., *et al*., Numerical study on optimization of ejector primary nozzle geometries. International Journal of Refrigeration, 2017. 76: p. 219-229. http://dx.doi.org/doi: 10.1016/j.ijrefrig.2017.02.010

[4] WB, G., Principle of refrigeration. 1982: Cambridge University Press. https://www.worldcat.org/title/principles-of-refrigeration/oclc/453028295

[5] Yapıcı, R., Experimental investigation of performance of vapor ejector refrigeration system using refrigerant R123. Energy Conversion and Management, 2008. 49(5): p. 953-961. http://doi.org/10.1016/j.enconman.2007.10.006

[20] Dong, J., *et al*., An Experimental Investigation of Steam Ejector Refrigeration Systems. Journal of Thermal Science and Engineering Applications, 2012. 4(3): p. 031004-031004-7. https://doi.org/10.1115/1.4006714

[6] Yapıcı, R. and H.K. Ersoy, Performance characteristics of the ejector refrigeration system based on the constant area ejector flow model. Energy Conversion and Management, 2005. 46(18): p. 3117-3135. http://doi.org/10.1016/j.enconman.2005.01.010

[7] Yapıcı, R., *et al*., Experimental determination of the optimum performance of ejector refrigeration system depending on ejector area ratio. International Journal of Refrigeration, 2008. 31(7): p. 1183-1189. http://doi.org/10.1016/j.ijrefrig.2008.02.010

[8] Yen, R.H., *et al*., Performance optimization for a variable throat ejector in a solar refrigeration system. International Journal of Refrigeration, 2013. 36(5): p. 1512-1520. http://doi.org/10.1016/j.ijrefrig.2013.04.005

[9] Arbel, A., *et al*., Ejector Irreversibility Characteristics. Journal of Fluids Engineering, 2003. 125(1): p. 121-129. http://doi.org/10.3390/en9030212

[10] B.ELHUB, MOHAMED AZLY ABDUL AZIZ, and MOHD KHAIRUL ANUAR BIN SHRIF SOHIF MAT, Review of ejector design parameters and geometry for refrigeration and air conditioning application. Computer Applications in Environmental Sciences and Renewable Energy, 2014.

[11] Besagni, G., R. Mereu, and F. Inzoli, Ejector refrigeration: A comprehensive review. Renewable and Sustainable Energy Reviews, 2016. 53: p. 373-407. https://doi.org/10.1016/j.rser.2015.08.059

[12] Chaiwongsa, P. and S. Wongwises, Experimental study on R-134a refrigeration system using a two-phase ejector as an expansion device. Applied Thermal Engineering, 2008. 28(5): p. 467-477. https://doi.org/10.1016/j.applthermaleng.2007.05.005

[13] Chandra, V.V. and M.R. Ahmed, Experimental and computational studies on a steam jet refrigeration system with constant area and variable area ejectors. Energy Conversion and Management, 2014. 79: p. 377-386. https://doi.org/10.1016/j.enconman.2013.12.035

[14] Chen, J., H. Havtun, and B. Palm, Investigation of ejectors in refrigeration system: Optimum performance evaluation and ejector area ratios perspectives. Applied Thermal Engineering, 2014. 64(1): p. 182-191. https://doi.org/10.1016/j.applthermaleng.2013.12.034

[15] Chen, W., *et al*., Theoretical analysis of ejector refrigeration system performance under overall modes. Applied Energy, 2017. 185: p. 2074-2084. https://doi.org/10.1016/j.apenergy.2016.01.103

[16] Chunnanond, K. and S. Aphornratana, Ejectors: applications in refrigeration technology. Renewable and Sustainable Energy Reviews, 2004. 8(2): p. 129-155. https://doi.org/10.1016/j.rser.2003.10.001

[17] Chunnanond, K. and S. Aphornratana, An experimental investigation of a steam ejector refrigerator: the analysis of the pressure profile along the ejector. Applied Thermal Engineering, 2004. 24(2): p. 311-322. https://doi.org/10.1016/j.applthermaleng.2003.07.003

[18] Dennis, M. and K. Garzoli, Use of variable geometry ejector with cold store to achieve high solar fraction for solar cooling. International Journal of Refrigeration, 2011. 34(7): p. 1626-1632. https://doi.org/10.1016/j.ijrefrig.2010.08.006

[19] Dong, J., *et al*., An experimental investigation of steam ejector refrigeration system powered by extra low temperature heat source. International Communications in Heat and Mass Transfer, 2017. 81(Supplement C): p. 250-256. https://doi.org/10.1016/j.icheatmasstransfer.2016.12.022

[21] Eames, I.W., S. Aphornratana, and H. Haider, A theoretical and experimental study of a small-scale steam jet refrigerator. International Journal of Refrigeration, 1995. 18(6): p. 378-386. https://doi.org/10.1016/0140-7007(95)98160-m

[22] Eames, I.W., *et al*., The design, manufacture and testing of a jet-pump chiller for air conditioning and industrial application. Applied Thermal Engineering, 2013. 58(1): p. 234-240. https://doi.org/10.1016/j.applthermaleng.2013.04.028

[23] Elbel, S. and N. Lawrence, Review of recent developments in advanced ejector technology. International Journal of Refrigeration, 2016. 62: p. 1-18. https://doi.org/10.1016/j.ijrefrig.2015.10.031

[24] Galanis, N. and M. Sorin, Ejector design and performance prediction. International Journal of Thermal Sciences, 2016. 104: p. 315-329. https://doi.org/10.1016/j.ijthermalsci.2015.12.022

[25] Grazzini, G., A. Milazzo, and D. Paganini, Design of an ejector cycle refrigeration system. Energy Conversion and Management, 2012. 54(1): p. 38-46. https://doi.org/10.1016/j.enconman.2011.09.015

[26] Hernandez, J.I., *et al*., The Behavior of an Ejector Cooling System Operating with Refrigerant Blends 410A and 507. Energy Procedia, 2014. 57: p. 3021-3030. https://doi.org/10.1016/j.egypro.2014.10.338

[27] Holtzapple, M.T., High-Efficiency Jet Ejector. Invention Disclosure, Texas A&M University, 2001.

[28] Huang, B.J., *et al*., A 1-D analysis of ejector performance. International Journal of Refrigeration, 1999. 22(5): p. 354-364. https://dx.doi.org/10.1016/S0140-7007(99)00004-3

[29] J.H. Keenan, E.P.N., F. Lustwerk, An Investigation of Ejector Design by Analysis and Experiment. Journal of Applied Mechanics, Trans.,ASME 1950. 72(299-309). http://dx.doi.org/10.1016/j.ijrefrig.2011.06.001

[30] Jia, Y. and C. Wenjian, Area ratio effects to the performance of air-cooled ejector refrigeration cycle with R134a refrigerant. Energy Conversion and Management, 2012. 53(1): p. 240-246. http://dx.doi.org/10.1016/j.enconman.2011.09.002

[31] Kong, F.S., *et al*., Application of Chevron Nozzle to a Supersonic Ejector–diffuser System. Procedia Engineering, 2013. 56(Supplement C): p. 193-200. http://dx.doi.org/10.1016/j.proeng.2013.03.107

[32] Li, F., *et al*., Experimental investigation on a R134a ejector refrigeration system under overall modes. Applied Thermal Engineering, 2018. 137: p. 784-791.

[33] Milazzo, A., A. Rocchetti, and I.W. Eames, Theoretical and Experimental Activity on Ejector Refrigeration. Energy Procedia, 2014. 45: p. 1245-1254. http://dx.doi.org/10.1016/j.egypro.2014.01.130

[34] Sait, H.H., *et al*., Fresnel-based modular solar fields for performance/cost optimization in solar thermal power plants: A comparison with parabolic trough collectors. Applied Energy, 2015. 141(Supplement C): p. 175-189. http://dx.doi.org/10.1016/j.apenergy.2014.11.074

[35] Ma, X., *et al*., Experimental investigation of a novel steam ejector refrigerator suitable for solar energy applications. Applied Thermal Engineering, 2010. 30(11): p. 1320-1325. http://dx.doi.org/10.1016/j.applthermaleng.2010.02.011

[36] Allouche, Y., C. Bouden, and S. Riffat, A Solar-Driven Ejector Refrigeration System for Mediterranean Climate: Experience Improvement and New Results Performed. Energy Procedia, 2012. 18: p. 1115-1124. http://dx.doi.org/10.1016/j.egypro.2012.05.126

[37] Göktun, S., Optimization of irreversible solar assisted ejector-vapor compression cascaded systems. Energy Conversion and Management, 2000. 41(6): p. 625-631.

[38] Gil, B. and J. Kasperski, Performance Analysis of a Solar-powered Ejector Air-conditioning Cycle with Heavier Hydrocarbons as Refrigerants. Energy Procedia, 2014. 57: p. 2619-2628. https://doi.org/10.1016/j.egypro.2014.10.273

[39] Bellos, Evangelos & Tzivanidis, Christos. (2017). Optimum design of a solar ejector refrigeration system for various operating scenarios. Energy Conversion and Management. 154. 10.1016/j.enconman.2017.10.057. https://doi.org/10.1016/j.egypro.2012.05.126

[40] Diaconu, B.M., Energy analysis of a solar-assisted ejector cycle air conditioning system with low temperature thermal energy storage. Renewable Energy, 2012. 37(1): p. 266-276. https://doi.org/10.1016/j.renene.2011.06.031

[41] Śmierciew, K., *et al*., Experimental investigations of solar driven ejector air-conditioning system. Energy and Buildings, 2014. 80: p. 260-267. https://doi.org/10.1016/j.enbuild.2014.05.033

Received on 24-11-2020 Accepted on 12-12-2020 Published on 23-12-2020

DOI: http://dx.doi.org/10.15377/2409-5818.2020.07.3

© 2020 Sait *et al*.; Avanti Publishers.
This is an open access article licensed under the terms of the Creative Commons Attribution Non-Commercial License (http://creativecommons.org/licenses/by-nc/3.0/) which permits unrestricted, non-commercial use, distribution and reproduction in any medium, provided the work is properly cited